FEBS Letters 587 (2013) 2150–2157

FEBS Letters

journal homepage: www.FEBSLetters.org

In vivo mutation of pre-mRNA processing factor 8 (Prpf8) affects transcript splicing, cell survival and myeloid differentiation

Maria-Cristina Keightley [a,1], Meredith O. Crowhurst [b,1], Judith E. Layton [b], Traude Beilharz [c], Sebastian Markmiller [b], Sony Varma [a,b], Benjamin M. Hogan [b], Tanya A. de Jong-Curtain [b,2], Joan K. Heath [b,2], Graham J. Lieschke [a,b,*]

[a] Australian Regenerative Medicine Institute, Monash University, Clayton, Victoria 3800, Australia
[b] Ludwig Institute for Cancer Research, Melbourne-Parkville Branch, The Royal Melbourne Hospital, Parkville, Victoria 3050, Australia
[c] Department of Biochemistry and Molecular Biology, Monash University, Clayton, Victoria 3800, Australia

ARTICLE INFO

Article history:
Received 22 October 2012
Revised 15 May 2013
Accepted 15 May 2013
Available online 25 May 2013

Edited by Ned Mantei

Keywords:
PRPF8
Haematopoiesis
Splicing
Zebrafish
Myelopoiesis
Spliceosome
snRNP

ABSTRACT

Mutated spliceosome components are recurrently being associated with perturbed tissue development and disease pathogenesis. *Cephalophŏnus* (*cph*), is a zebrafish mutant carrying an early premature STOP codon in the spliceosome component Prpf8 (pre-mRNA processing factor 8). *Cph* initially develops normally, but then develops widespread cell death, especially in neurons, and is embryonic lethal. *Cph* mutants accumulate aberrantly spliced transcripts retaining both U2- and U12-type introns. Within early haematopoiesis, myeloid differentiation is impaired, suggesting Prpf8 is required for haematopoietic development. *Cph* provides an animal model for zygotic PRPF8 dysfunction diseases and for evaluating therapeutic interventions.

1. Introduction

There is mounting evidence that regulation of pre-mRNA splicing is critical for correct lineage specification in haematopoiesis [1–4]. Spliceosomes are composed of uridine-rich small nuclear ribonucleoprotein particles (U-snRNPs) and multiple associated proteins. The vast majority of introns in pre-mRNA are excised by U2-dependent major spliceosomes, which contain U1, U2, U4/U6 and U5 snRNPs. PRPF8 (pre-mRNA processing factor 8) is a highly conserved component of both major and U12-dependent minor spliceosomes [5,6] with 98% sequence identity between human and zebrafish proteins. PRPF8 amino acid region 437–770 binds several U5 snRNP proteins [7,8] and the C-terminal is required for activation of Brr2 helicase unwinding of the U4/U6 duplex essential for catalytic activation of the spliceosome [9,10]. It has recently been shown that the RNase H region that binds Brr2 also binds U4/U6 [11,12].

The recent identification of recurrent mutations in spliceosome components in myelodysplastic syndromes (MDS) and MDS-related secondary leukaemias in multiple genome-wide sequencing surveys has attracted considerable interest, both for their potential functional role in MDS pathogenesis, and for their prognostic significance [13,14]. An MDS-associated PRPF8 allele has recently been reported, occurring in a patient with MDS-related secondary leukaemia [15]. A cluster of varied carboxyl-terminal PRPF8 mutations has previously been implicated in autosomal dominant retinitis pigmentosa [16].

From a forward genetic chemical screen in zebrafish, a mutant named *Cephalophŏnus* (*cph*) was recovered and shown by positional cloning to carry a premature stop codon in Prpf8 predicted to result in a Prpf8-null phenotype. Mutation of this large protein at the centre of the spliceosome results in pleiotropic phenotypes that include neural degeneration and defective early haematopoiesis, with myelopoiesis more perturbed than erythropoiesis at

* Corresponding author at: Australian Regenerative Medicine Institute, Level 1, Building 75, Monash University, Clayton, Victoria 3800, Australia. Fax: +61 3 9902 9729.
E-mail address: Graham.Lieschke@monash.edu (G.J. Lieschke).
[1] These authors contributed equally to this work.
[2] Current address: The Walter & Eliza Hall Institute of Medical Research, Parkville, Victoria 3052, Australia.

0014-5793/$36.00
http://dx.doi.org/10.1016/j.febslet.2013.05.030

32 h post fertilisation (hpf). *Cph* mutants exhibit aberrant splicing that, at least initially, does not affect all genes uniformly.

2. Materials and methods

2.1. Zebrafish

Strains: St Kilda Wild Type (SKWT; local pet shop, St Kilda, Vic., Aust.), WIK, AB, AB* (Zebrafish International Research Centre, Eugene, Oregon, USA) and Tübingen (Max-Planck-Institut für Entwicklungsbiologie, Tübingen, Germany). *Cephalophŏnus* (*cph*^{gl1}) is a novel mutant isolated from an ethylnitrosourea (ENU) mutagenesis screen [17]. Fish were housed in the Ludwig Institute for Cancer Research Aquarium and ARMI FishCore using standard husbandry practices. All experiments were approved by the Ludwig Institute for Cancer Research or Monash University Animal Ethics Committees.

2.2. Microinjections

Fertilised 1- to 2-cell embryos were microinjected with *prpf8* splice site morpholino oligonucleotide (250 μM in H_2O; Gene Tools, Philomath, OR); or control MO (see Table S2 for sequence), (250 μM in H_2O; Gene Tools) traced where appropriate by mixing 1:1 with 5% rhodamine–dextran.

2.3. Positional cloning

The genomic scan was performed in the laboratory of Dr. L. Zon (Children's Hospital, Boston, MA, USA), by Dr. J. Layton, under the guidance of Helen Foote and Yi Zhou. A 10 cM scan was performed against a panel of SSLP (simple sequence length polymorphism) markers, which placed *cph* on chromosome 15. The region was subsequently narrowed using RFLP (restriction fragment length polymorphism) markers and SNP (single nucleotide polymorphism) analysis. The Zv7 genome scaffold used as a mapping reference was incorrectly assembled in this region. Supplementary Table S2 lists oligonucleotide sequences used.

2.4. Acridine orange staining

Acridine orange (AO) staining was performed as described [18] and modified [19]. Embryos were viewed on a Bio-Rad MRC-1024 laser scanning confocal microscope at 2 h intervals between 12 h post fertilisation (hpf) and 36 hpf. Images were processed using LaserSharp2000 software.

2.5. Gene expression analysis

Whole mount *in situ* hybridisation (WISH) was performed using standard techniques [20]. For antibody staining details refer to Supplementary methods. Whole embryos were visualised using a Leica MZ6 stereo dissecting light microscope (Leica Microsystems, Gladesville, N.S.W., Aust.). Anti-active caspase 3 immunofluorescence was detected by Alexafluor-conjugated secondary antibody (Molecular Probes) and confocal microscopy as in Section 2.4.

2.6. Histology

Embryos for sectioning and staining were fixed o/n in 4% paraformaldehyde, embedded in 1% Bacto-Agar (DIFCO) and stored in 70% ethanol before out-sourcing to the histology unit at the Walter and Eliza Hall Institute, Parkville, Victoria, Aust. Embryos were sectioned (transverse or sagittal) at 3 μm intervals, stained with haematoxylin and eosin and viewed on a Nikon Microphot FX upright compound microscope. Images were captured with a SPOT-1 cooled CCD digital camera (Diagnostic Instruments Inc., Sterling Heights, MI, USA).

2.7. Genotyping

From 28 hpf, *cph* embryos were readily recognised in a Mendelian proportion by their pleiotropic phenotypes including small eyes, disrupted neural region, lack of ventricle inflation, and thinner yolk extension. Younger *cph* embryos were genotyped by PCR using exon 8 primers (oligonucleotides, Table S2; 20 μl reactions; Phusion polymerase [New England Biolabs, MA] with supplied GC buffer; 95 °C, 2 min followed by 45 cycles at 95, 60 °C, and for 30, 30, and 60 s, respectively, and 1 cycle of 10 min at 72 °C; PCR products were gel purified, then sequenced).

2.8. Preparation of embryo extracts, glycerol gradient centrifugation and northern blotting

Extracts from 2 dpf larvae were prepared in buffer G (20 mM HEPES, adjusted to pH 7.9 with KOH, 150 mM KCl, 1.5 mM $MgCl_2$, 1 mM DTT, 0.5 mM PMSF, 0.02% NP40) + 8% glycerol, layered onto 10–30% glycerol gradients in buffer G and centrifuged for 19 h at 39 500 rpm in an SW40 rotor at 4 °C in an Optima L-90K ultracentrifuge (Beckman Coulter). Samples were separated into 20 fractions. RNA was extracted by phenol–chloroform and separated by electrophoresis on 10% polyacrylamide/8 M urea–TBE gels. After transfer of nucleic acids to Hybond-N nylon membrane (GE Healthcare), membranes were hybridised with ^{32}P-radiolabelled probes to zebrafish U2, U4, U5, U6, U11 and U12 snRNAs (Table S2).

2.9. Splicing analysis by RT-PCR

WT and sibling mutant embryos were harvested at 48 hpf in Trizol. Total RNA was isolated and cDNA synthesised by standard methods. PCR was performed: 98 °C, 30 s; [98 °C, 30 s; 65 °C (60 °C for exon skipping), 15 s; 72 °C, 30 s] × 30; 72 °C, 7 min, using splice site primers as described [21,22].

3. Results

3.1. Loss of Prpf8 results in neural degeneration due to apoptosis

Cephalophŏnus (*cph*) is a recessive zebrafish mutant recovered from an ENU forward genetics screen for myeloid defects. Under bright field microscopy, gross morphology of homozygous mutants appears normal until 28 hpf after which time the entire brain and spinal cord become opaque due to widespread cell death throughout the central nervous system (Fig. 1A). The embryos develop kyphosis, and display a twitch in response to touch stimuli (Fig. 1C). Despite this extensive cell death, development continues, but over the next 48 hpf, the whole embryo progressively degenerates. Circulatory defects are accompanied by increasing pericardial oedema (Fig. 1D) and mutants die by 96 hpf.

Staining by acridine orange, a marker of cell death, from 12 to 28 hpf (Fig. 1E) showed cells positive for acridine orange uptake were initially scattered similarly throughout both wild type and mutant embryos at 12–14 hpf. Their relative abundance progressively diminished in WT embryos but markedly increased in *cph* mutants with an anatomically unconstrained distribution, indicating a general effect on undifferentiated neuroepithelium as well as multiple other cell types. Immunostaining for active caspase-3 recapitulated the pattern of acridine orange staining (Fig. 1F), suggesting that the mechanism of extensive cell death in *cph* embryos involves apoptosis.

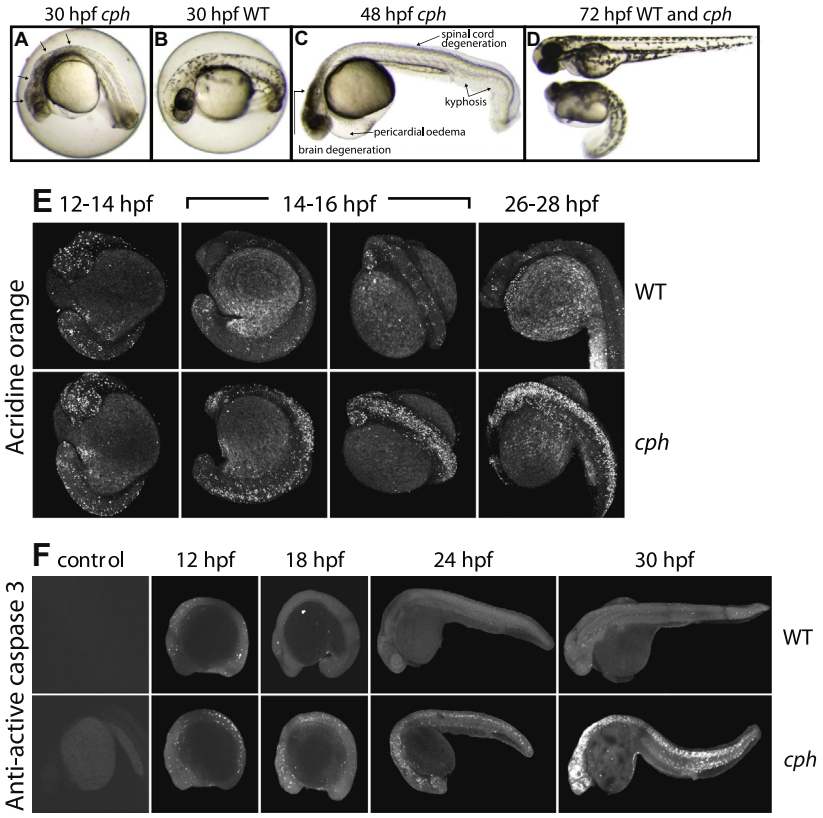

Fig. 1. Neuronal cell death in *cph* occurs via apoptosis. (A–D) are bright field microscopy. (A) *Cph* 30 hpf embryos display cranial opacity (arrows), indicative of CNS degeneration, compared to WT siblings (B). (C) At 48 hpf, *cph* develop severe pericardial oedema and curvature of the spine (kyphosis). (D) At 72 hpf, *cph* (below) are much smaller than age-matched WT (above), with weak heart beat and circulation. (E) WT (above) and *cph* mutant sibling (below) from 12 to 28 hpf. *Cph* shows a marked excess of cells with nuclear uptake of acridine orange compared to WT from 14 to 16 hpf, most predominantly in the neuraxis; and (F) Anti-active caspase 3 staining in WT (above) and *cph* mutant sibling (below) from 12 to 30 hpf, demonstrating increased number of apoptotic cells in *cph*.

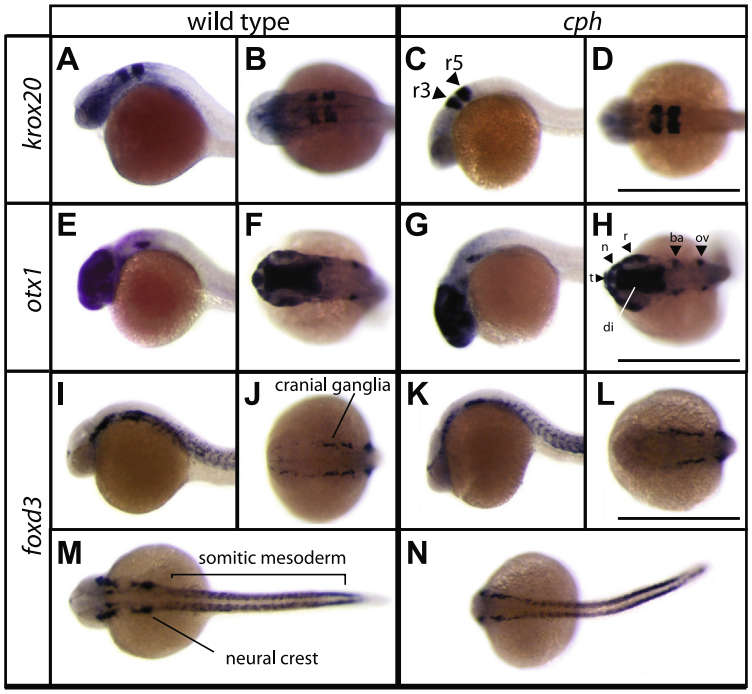

Fig. 2. Neural patterning and specification occurs in *cph*. Whole mount in situ hybridisation at 30 hpf (A–H) and 28 hpf (I–N) showing similar staining patterns for WT and *cph* indicating neural specification occurs normally for *krox20* (A–D), *otx1* (E–H), and *foxd3* (I–N) lineages. Alternating lateral and dorsal views, anterior to the left (A–L). (M–N), dorsal. *R3*, *r5*, hindbrain rhombomeres; *t*, telencephalon; *di*, diencephalon; *n*, nose; *r*, retina; *ba*, brachial arches; *ov*, otic vesicles.

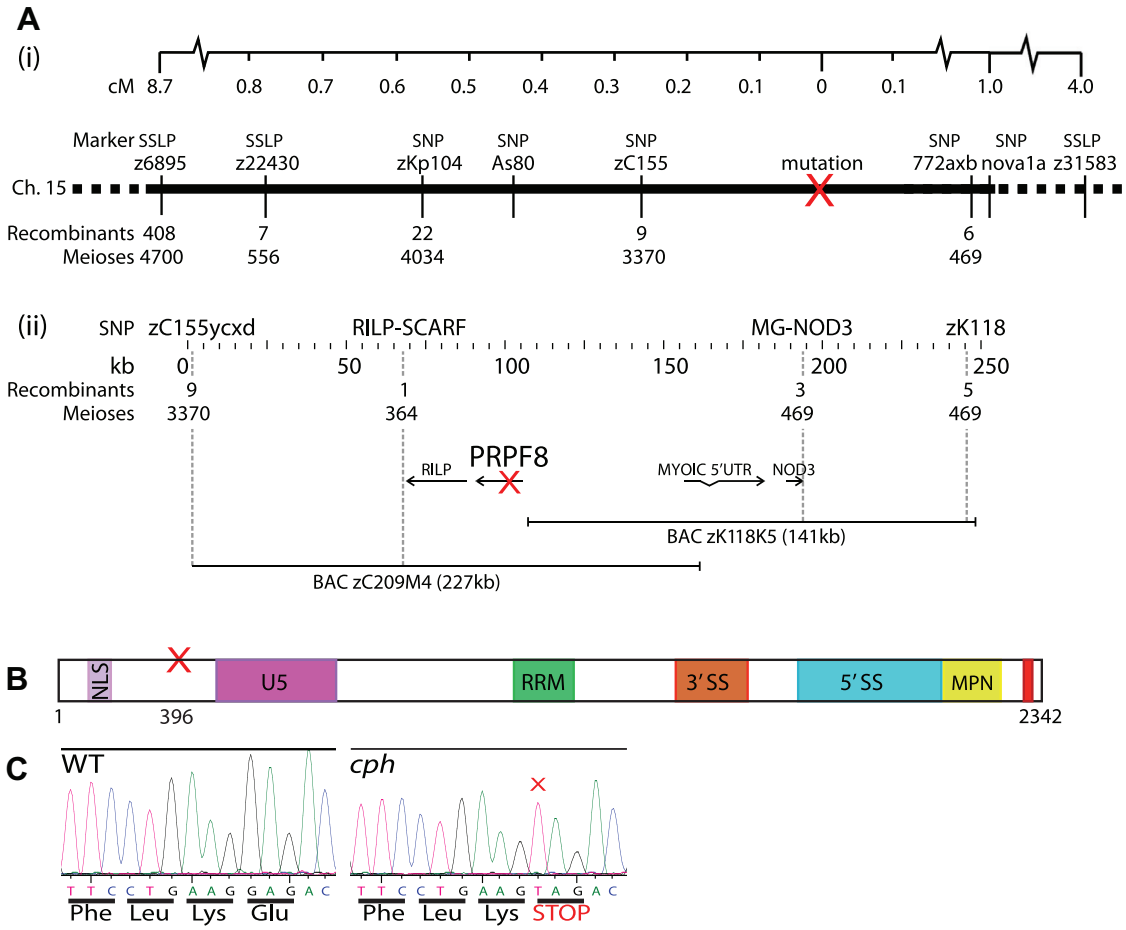

Fig. 3. Positional cloning of *cph* gene, *prpf8*. Panel A (i) Genetic map; cM, centimorgans; SSLP, simple sequence length polymorphism; SNP, single-nucleotide polymorphism. (ii) Physical map containing the critical interval with four candidate genes: *nod3* (Nucleotide-binding oligomerisation domain), *myo1c* (Myosin1c), *prpf8*, and *rilp* (Rab interacting lysosomal protein); (B) schematic of Prpf8 protein with *cph* mutation shown by red cross. Sequence motifs that are likely to have functional roles are shown: NLS, nuclear localisation signal; U5, U5 binding site; RRM, RNA recognition motif; 5′SS, 5′ splice site fidelity; 3′SS, 3′ splice site fidelity; MPN, Mpr-1, Pad-1, N-terminal domain; site of retinitis pigmentosa mutations indicated by red bar. (C) Sequence chromatograph, with *cph* E396X mutation in red; cross marks the G > T transversion.

3.2. Prpf8 is not required for initiation of neural lineage patterning and specification

Despite widespread neural cell death, *cph* brains showed evidence of normal neural induction, morphogenesis and regionalisation with formation of specific structures (Fig. S1A–D). Neuronal specification and differentiation also proceeded in *cph* with surprising normality at 28–30 hpf (Fig. 2; Table S1). Together, these data indicate that, neuronal cell death notwithstanding, early neural patterning and specification were able to proceed in *cph* embryos.

3.3. A premature stop mutation in prpf8 underpins cephalophõnus

A genomic scan positioned the *cph* mutation on chromosome 15. Intermediate mapping confined the mutation to within a 4.5 cM interval between SSLP markers z22430 and z31583. Recombinants identified using SNP and RFLP markers that were developed in the interval and a mapping panel totalling 4,700 informative meioses narrowed the genetic interval to 4 genes (Fig. 3A, i and ii). One of these genes, *prpf8*, was a likely candidate on several grounds including its ubiquitous expression pattern [23,24] and that it is a component of the spliceosome and toposome. Defects in genes involved in RNA processing are known to cause central nervous system (CNS) degeneration in zebrafish mutants [25–27]. *Prpf8* cDNAs were cloned and sequenced from *cph* mutant and wild-type embryos, and a G > T transversion was identified in exon 8 (out of 42) which changed E396 into a premature stop codon (GAG > TAG) (Fig. 3B and C). The G > T mutation was not present in the somatic DNA of the ENU-treated founder from which *cph* was derived, confirming it was ENU-induced.

Given the *prpf8* cDNA predicts a full-length protein of 2342 amino acids, truncation of such a large and highly conserved protein to 395 amino acids is likely a null mutation, and therefore a strong candidate for the causative mutation. The causality of the *prpf8* mutation was supported by phenocopy of *cph* following *prpf8* knockdown in WT embryos using a morpholino antisense oligonucleotide targeted to the first exon/intron splice site in *prpf8*. Increased acridine orange staining was observed in 94% (67/71) of injected embryos, compared to 0% of control (non-injected) embryos and 0% of control morpholino injected embryos.

3.4. Myeloid development requires Prpf8

Recurrent mutations in spliceosome components including PRPF8 have recently been identified in myelodysplastic syndromes prompting a survey of the expression of haematopoietic marker genes in *cph* at 28 hpf by whole mount *in situ* hybridisation (WISH). Myelomonocytic markers were all reduced in *cph* compared to WT siblings (Fig. 4A–F). In contrast, expression of the haemoglobin component gene, *hbae3*, and o-dianisidine stain-

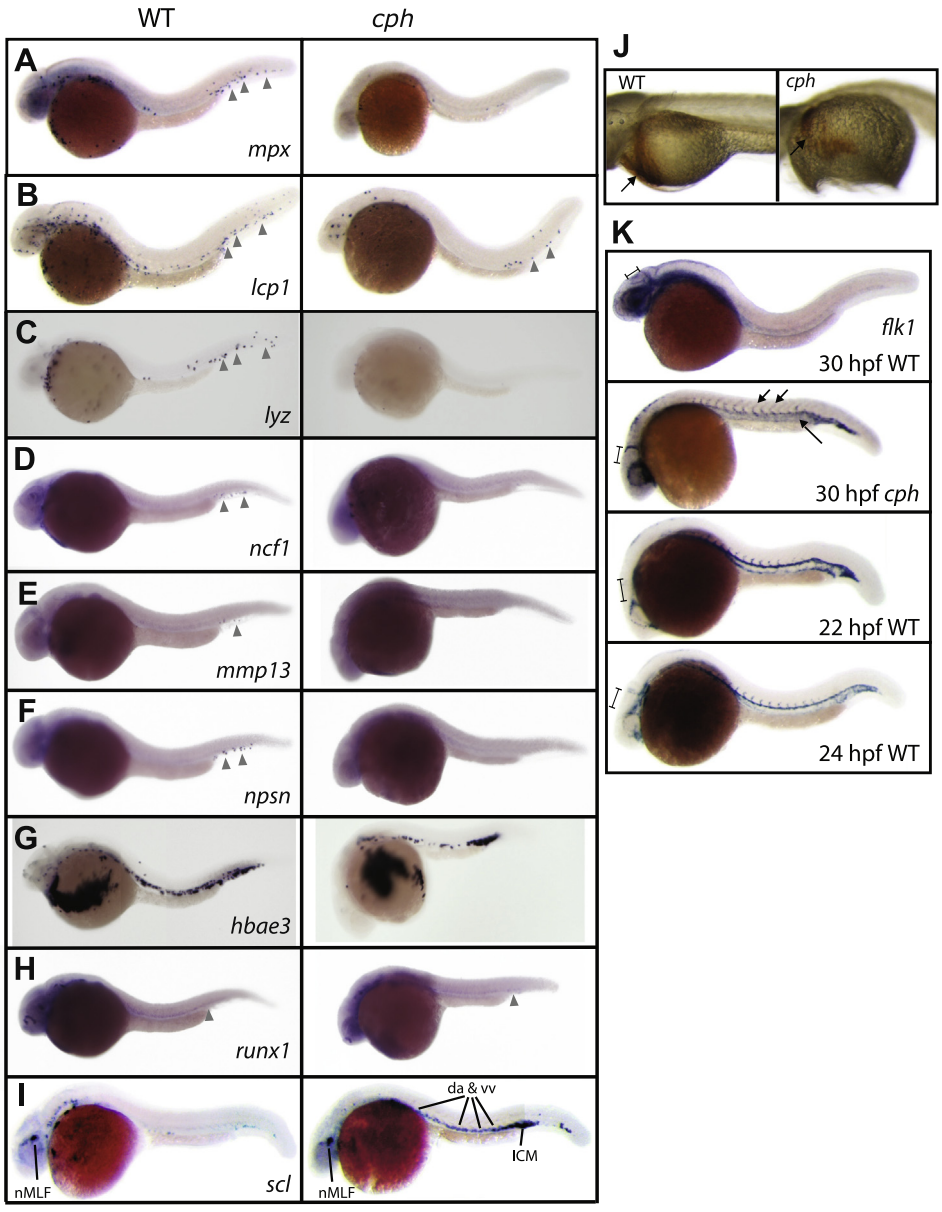

Fig. 4. Erythrocytes appear normal in *cph* but myeloid development is affected. A-I are whole mount *in situ* hybridisation (WISH) gene expression analyses with myelomonocytic (A–F), erythroid (G), *runx1* (H) *scl* (I) markers. (J) is o-dianisidine staining of haemoglobin. (K) *flk1* WISH analysis of developing endothelium; bracket indicates the distance between the aortic arch and developing eye. WT and *cph* embryos were collected at: A–H, 28 hpf; I, 72 hpf; J, 3dpf. nMLF, nucleus of the medial longitudinal fasciculus; isv, intersomitic vesicle; da, dorsal aorta; vv, ventral vein; ICM, intermediate cell mass.

ing of haemoglobin protein in erythrocytes appeared similar between WT and mutant (Fig. 4G and J) suggesting that myeloid cell development may be initially more dependent on zygotic *prpf8* transcription than erythropoiesis. Interestingly, the master haematopoietic regulator *scl* was ectopically expressed in *cph* mutants compared to WT siblings (Fig. 4I). By 28 hpf, WT *scl* expression is restricted to neural progenitor populations within the brain (e.g. nMLF). *cph* mutants, however, retain strong expression of *scl* in the hematopoietic regions at 28 hpf, where *scl* marks blood and vascular-fated cells in the region of the emergent dorsal aorta and intermediate cell mass (ICM). Although this pattern is reminiscent of that seen in younger 24 hpf WT embryos, in *cph* there is striking concurrent normal expression of *scl* in the nMLF at 28 hpf which has not yet initiated in 24 hpf WT siblings. *Flk1*, marking the endothelium, is also aberrantly strongly expressed in the developing trunk and intersomitic vessels at 30 hpf in *cph* (Fig. 4K).

3.5. Splicing defects occur in cph mutants

To determine if the spliceosome was functional in *prpf8* mutants, splicing of pre-mRNA molecules was assessed by RT-PCR across a range of genes previously characterised for splicing aberrations in other published studies [1,28–30] including haematopoietic (*gata1*, *hbbe1*, *mpx*, *mmp9*), signalling (*mapk3*, *mapk8*, *mapk12*), tumour suppressor (*p53*), and housekeeping (*tubulin*) genes. At 48 hpf, *cph* showed accumulation of transcripts retaining both major and/or minor class introns for the erythroid gene *gata1*, for *mapk12* and *p53* but not *tubulin* (Fig. 5A and B). When *cph* was assessed for splicing of its *prpf8* mutant transcript, intron 7–8 was retained (Fig. 5A). Further splicing analysis in haematopoietic genes revealed an inverse proportion of exon 1/2/3/4 transcripts versus exon 1/3/4 splice variants for the myeloid gene *spi1* indicating exon 2 is moreoften skipped in *cph* compared to WT (Fig. 5C). Exon skipping was also observed to a lesser degree for *gata1* but not for

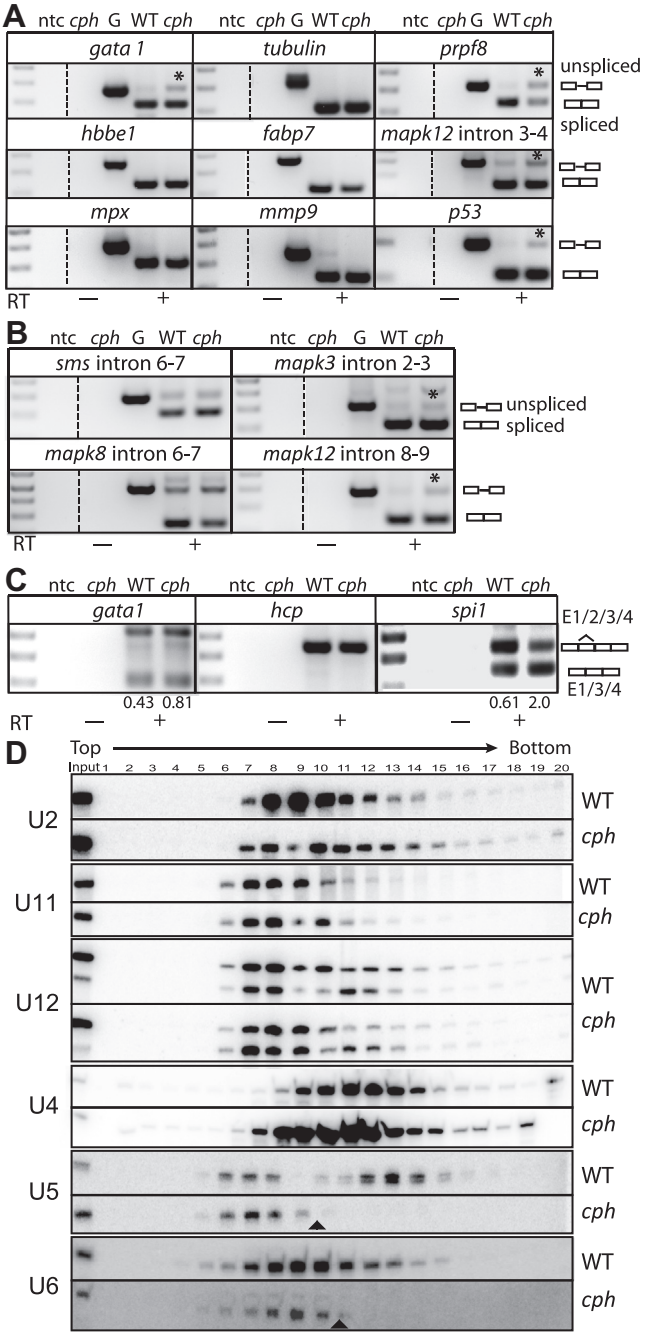

Fig. 5. Splicing and snRNP assembly is impaired in *cph* mutants. Semi-quantitative RT-PCR using template prepared from 48 hpf embryos and primers that span U2-type (A) U12-type (B) introns ⩽ 300 bp and alternatively spliced exons (C); numbers in *gata1* and *spi1* refer to proportion of exon-skipped versus non-skipped transcripts (ImageJ). NTC, no template control; G, genomic DNA; *cph*, *cph* mutant, WT, wild-type; RT, reverse transcriptase; (+) plus RT; (−) minus RT. Asterisks (∗) mark intron retention. (D) Northern analysis of glycerol gradient fractionation for U2, U11, U12, U4, U5 and U6 snRNAs in WT and *cph* extracts. Direction of the gradient is marked, fractions are numbered, solid triangles mark drop-off in *cph* fractions.

haematopoietic cell phosphatase (*hcp*). Sedimentation profiling of U2, U11 and U12 snRNAs of the major and minor spliceosomes and U4 snRNA revealed no differences between *cph* and WT. Analysis of U5 and U6 profiles showed that these snRNAs are present in both WT and *cph*, however, *cph* U5 and U6 are not associated with the higher molecular weight complexes seen in WT profiles suggesting that C-terminal truncation of Prpf8 interferes with tri-snRNP assembly (Fig. 5D).

4. Discussion

It is increasingly evident that regulation of pre-mRNA splicing events is crucial in correct haematopoietic lineage specification [1–4]. New in vivo models are needed to dissect the mechanisms and cell biological consequences of splicing dysfunction. *Cph* represents such a model. Four lines of evidence are consistent with *cph* being a chemically-induced *prpf8* loss-of-function mutation: tight genetic linkage demonstrated by formal positional cloning and non-segregation through multi-generational pedigree maintenance of >21 generations; phenotype phenocopy by *prpf8* knockdown; the *prpf8* mutation was introduced by ENU as it was not in the somatic tissue of the mutated male; and biochemical confirmation of a consequential splicing defect. Although further genetic evidence could be contributed by non-complementation with an independent *prpf8* allele, this is as yet unavailable.

The *cph* model of Prpf8 function shows pleiotropic phenotypes that include neural degeneration accompanied by defects in myelopoiesis and transcript splicing. Caspase-3 activation implicates apoptosis in the degenerative process in *cph*. Further studies are required to understand the precise nature and kinetics of cell death in *cph*. Of note, in *cph*, neural patterning and neuron specification proceed at a normal developmental pace, independently of the ongoing cell death, which is likely due to interruption of a widespread cell process necessary for neural cell survival. In contrast, in the haematopoietic compartment, there may be lineage specific defects at the time points examined. The aberrantly strong expression of *scl* in the hematopoietic regions of *cph* at 28 hpf suggests a requirement for a Prpf8-dependent product in coordinating its tight temporal down-regulation. *Scl* is essential for the normal development of primitive and definitive haematopoietic lineages in zebrafish [31] and the prolonged *scl* expression in *cph* would be expected to expand all haematopoietic lineages. However, in *cph*, decreased expression of myeloid lineage markers compared to erythroid markers was observed at 32 hpf. Hence, effective spatio-temporal splicing may be more important for a myelopoiesis-specific cofactor(s), and/or downstream pre-mRNA regulatory processes may preclude an *scl*-driven myeloid expansion more so than erythroid cell specification and survival.

Prpf8 C-terminal contacts several U5 snRNP proteins and is indispensible for activation of Brr2-dependent unwinding of the U4/U6 duplex required for spliceosome catalytic function [7–9]. The aberrant U5 and U6 sedimentation data suggesting the failure of U4/6·U5 tri-snRNP formation in *cph in vivo*, are consistent with *in vitro* studies underscoring the importance of Prpf8 in spliceosome assembly. U4 snRNA higher molecular weight complexes form in *cph* however the exact snRNP composition of these is not known.

Aberrant splicing of transcripts is evident in *cph* but not uniform for all genes. For a number of haematopoietic and housekeeping genes, splicing in *cph* was indistinguishable from WT. Zebrafish have an advantage over mice in that the maternal to zygotic transition occurs later in development allowing for analyses of cell-essential genes [32]. This maternal contribution can initially rescue a loss-of-function phenotype prior to destabilisation of maternal transcripts and onset of zygotic genome activation. Strong expression of zebrafish *prpf8* prior to the mid blastula transition indicates maternal *prpf8* mRNA deposition [23,24]. Differential persistence of enough maternal Prpf8 protein and transcript in some cell types rather than others together with wide-ranging variation in transcript stability between genes/cells could account for the differential gene splicing observed in *cph*. In addition, permanently retained introns are degraded very efficiently by the nuclear exosome either via non-sense mediated decay (NMD) or independently of it [33], although treatment of embryos with cycloheximide to block NMD did not result in increased

accumulation of aberrantly spliced transcripts in *cph* in any of the 12 genes tested (data not shown).

Splicing of Prpf8 itself is defective in *cph*. The aberrant transcript retains intron 7–8 introducing a stop codon 26 amino acids downstream of exon 7 prior to the mutation-encoded premature termination codon in exon 8, further compounding the defects in *cph* Prpf8. This suggests Prpf8 is involved in splicing of its own pre-mRNA and may point to an auto-regulatory feedback mechanism. That splicing defects are not seen in all genes in *cph* suggests a subset of pre-mRNAs, including *prpf8* itself, that rely particularly on Prpf8 to strengthen U5/exon interactions necessary for splicing [34]. It is also possible that Prpf8 functions outside of its role in the spliceosome to generate the *cph* phenotype. Full transcriptional profiling using RNAseq would more accurately determine the percentage of genes carrying unspliced versus spliced or alternatively spliced transcripts in *cph* and provide quantitative information on spliced versus unspliced transcripts for a given gene.

Several elegant precedents illustrate the utility of zebrafish for studying spliceosomal protein dysfunction biochemically [35–37] and as it relates to human disease [25,38–40]. Similarly, knockdown of *prpf8* in zebrafish and rescue of *cph* mutants will provide new tools with which to study Prpf8 protein function and a platform for understanding pre-mRNA splicing that will contribute to a better molecular understanding of spliceosome function. Once the technical challenges are overcome, a genetic complementation assay for human PRPF8 allele function can be developed as a vertebrate model for understanding the molecular pathogenesis of PRPF8-associated diseases, retinitis pigmentosa and myelodysplastic syndromes (MDS). This will present a whole-organism system for evaluating potential therapeutic interventions.

Acknowledgments

We thank: M. Greer, K. Turner and P. Chamberlain for animal care; S. Jane, D. Curtis and the Royal Melbourne Hospital Bone Marrow Research laboratory for support. This work was supported by Grants to G.J.L. from NIH (RO1 HL079545), the NHMRC (234708, 461208, 516750, 637395) and ARC (DP0346823). MOC was supported by an Australian Postgraduate Award. The Australian Regenerative Medicine Institute is supported by grants from the State Government of Victoria and the Australian Government.

Appendix A. Supplementary data

Supplementary data associated with this article can be found, in the online version, at http://dx.doi.org/10.1016/j.febslet.2013.05.030.

References

[1] English, M.A., Lei, L., Blake, T., Wincovitch Sr., S.M., Sood, R., Azuma, M., Hickstein, D. and Paul Liu, P. (2012) Incomplete splicing, cell division defects and hematopoietic blockage in dhx8 mutant zebrafish. Dev. Dyn. 241, 879–889.
[2] Liu, P., Barb, J., Woodhouse, K., Taylor, J.G.T., Munson, P.J. and Raghavachari, N. (2011) Transcriptome profiling and sequencing of differentiated human hematopoietic stem cells reveal lineage-specific expression and alternative splicing of genes. Physiol. Genom. 43, 1117–1134.
[3] Bedi, R., Du, J., Sharma, A.K., Gomes, I. and Ackerman, S.J. (2009) Human C/EBP-epsilon activator and repressor isoforms differentially reprogram myeloid lineage commitment and differentiation. Blood 113, 317–327.
[4] Yamamoto, M.L., Clark, T.A., Gee, S.L., Kang, J.A., Schweitzer, A.C., Wickrema, A. and Conboy, J.G. (2009) Alternative pre-mRNA splicing switches modulate gene expression in late erythropoiesis. Blood 113, 3363–3370.
[5] Grainger, R.J. and Beggs, J.D. (2005) Prp8 protein: at the heart of the spliceosome. RNA 11, 533–557.
[6] Luo, H.R., Moreau, G.A., Levin, N. and Moore, M.J. (1999) The human Prp8 protein is a component of both U2- and U12-dependent spliceosomes. RNA 5, 893–908.
[7] Boon, K.L., Grainger, R.J., Ehsani, P., Barrass, J.D., Auchynnikava, T., Inglehearn, C.F. and Beggs, J.D. (2007) Prp8 mutations that cause human retinitis pigmentosa lead to a U5 snRNP maturation defect in yeast. Nat. Struct. Mol. Biol. 14, 1077–1083.
[8] Boon, K.L., Norman, C.M., Grainger, R.J., Newman, A.J. and Beggs, J.D. (2006) Prp8p dissection reveals domain structure and protein interaction sites. RNA 12, 198–205.
[9] Maeder, C., Kutach, A.K. and Guthrie, C. (2009) ATP-dependent unwinding of U4/U6 snRNAs by the Brr2 helicase requires the C terminus of Prp8. Nat. Struct. Mol. Biol. 16, 42–48.
[10] Weber, G. et al. (2013) Structural basis for dual roles of Aar2p in U5 snRNP assembly. Genes Dev. 27, 525–540.
[11] Mozaffari-Jovin, S., Santos, K.F., Hsiao, H.H., Will, C.L., Urlaub, H., Wahl, M.C. and Luhrmann, R. (2012) The Prp8 RNase H-like domain inhibits Brr2-mediated U4/U6 snRNA unwinding by blocking Brr2 loading onto the U4 snRNA. Genes Dev. 26, 2422–2434.
[12] Galej, W.P., Oubridge, C., Newman, A.J. and Nagai, K. (2013) Crystal structure of Prp8 reveals active site cavity of the spliceosome. Nature 493, 638–643.
[13] Abdel-Wahab, O. and Levine, R. (2011) The spliceosome as an indicted conspirator in myeloid malignancies. Cancer Cell 20, 420–423.
[14] Hahn, C.N. and Scott, H.S. (2012) Spliceosome mutations in hematopoietic malignancies. Nat. Genet. 44, 9–10.
[15] Makishima, H. et al. (2012) Mutations in the spliceosome machinery, a novel and ubiquitous pathway in leukemogenesis. Blood 119, 3203–3210.
[16] Towns, K.V. et al. (2010) Prognosis for splicing factor PRPF8 retinitis pigmentosa, novel mutations and correlation between human and yeast phenotypes. Hum. Mutat. 31, E1361–E1376.
[17] Hogan, B.M. et al. (2006) Specification of the primitive myeloid precursor pool requires signaling through Alk8 in zebrafish. Curr. Biol. 16, 506–511.
[18] Furutani-Seiki, M. et al. (1996) Neural degeneration mutants in the zebrafish, *Danio rerio*. Development 123, 229–239.
[19] Rodriguez, M. and Driever, W. (1997) Mutations resulting in transient and localized degeneration in the developing zebrafish brain. Biochem. Cell Biol. 75, 579–600.
[20] Lieschke, G.J. et al. (2002) Zebrafish SPI-1 (PU.1) marks a site of myeloid development independent of primitive erythropoiesis: implications for axial patterning. Dev. Biol. 246, 274–295.
[21] Payne, E.M. et al. (2011) Ddx18 is essential for cell cycle progression in zebrafish hematopoietic cells and is mutated in human acute myeloid leukemia. Blood 118, 903–915.
[22] Konig, H., Matter, N., Bader, R., Thiele, W. and Muller, F. (2007) Splicing segregation: the minor spliceosome acts outside the nucleus and controls cell proliferation. Cell 131, 718–729.
[23] Kudoh, T., Tsang, M., Hukriede, N.A., Chen, X., Dedekian, M., Clarke, C.J., Kiang, A., Schultz, S., Epstein, J.A., Toyama, R. and Dawid, I.B. (2001) A gene expression screen in zebrafish embryogenesis. ZFIN Direct Data Submission <http://zfin.org>.
[24] Thisse, B. and Thisse, C. (2004) Fast release clones: a high throughput expression analysis. ZFIN Direct Data Submission <http://zfin.org>.
[25] Linder, B. et al. (2011) Systemic splicing factor deficiency causes tissue-specific defects: a zebrafish model for retinitis pigmentosa. Hum. Mol. Genet. 20, 368–377.
[26] Winkler, C., Eggert, C., Gradl, D., Meister, G., Giegerich, M., Wedlich, D., Laggerbauer, B. and Fischer, U. (2005) Reduced U snRNP assembly causes motor axon degeneration in an animal model for spinal muscular atrophy. Genes Dev. 19, 2320–2330.
[27] Yin, J., Brocher, J., Fischer, U. and Winkler, C. (2011) Mutant Prpf31 causes pre-mRNA splicing defects and rod photoreceptor cell degeneration in a zebrafish model for *Retinitis pigmentosa*. Mol. Neurodegener. 6, 56.
[28] Wutz, D., Shayan, P., Schmahl, G.E., Mild, G.C., Feil, B., Roll, S., Kontny, H.U. and Niemeyer, C.M. (1999) Gene expression of the hematopoietic cell phosphatase in juvenile myelomonocytic leukemia. Leuk. Lymphoma 35, 491–499.
[29] Rainis, L. et al. (2003) Mutations in exon 2 of GATA1 are early events in megakaryocytic malignancies associated with trisomy 21. Blood 102, 981–986.
[30] Ward, A.C. et al. (2003) The zebrafish spi1 promoter drives myeloid-specific expression in stable transgenic fish. Blood 102, 3238–3240.
[31] Dooley, K.A., Davidson, A.J. and Zon, L.I. (2005) Zebrafish scl functions independently in hematopoietic and endothelial development. Dev. Biol. 277, 522–536.
[32] Tadros, W. and Lipshitz, H.D. (2009) The maternal-to-zygotic transition: a play in two acts. Development 136, 3033–3042.
[33] Parker, R. (2012) RNA degradation in *Saccharomyces cerevisiae*. Genetics 191, 671–702.
[34] Aronova, A., Bacikova, D., Crotti, L.B., Horowitz, D.S. and Schwer, B. (2007) Functional interactions between Prp8, Prp18, Slu7, and U5 snRNA during the second step of pre-mRNA splicing. RNA 13, 1437–1444.
[35] Trede, N.S. et al. (2007) Network of coregulated spliceosome components revealed by zebrafish mutant in recycling factor p110. Proc. Natl. Acad. Sci. USA 104, 6608–6613.
[36] Rosel, T.D., Hung, L.H., Medenbach, J., Donde, K., Starke, S., Benes, V., Ratsch, G. and Bindereif, A. (2011) RNA-Seq analysis in mutant zebrafish reveals role of U1C protein in alternative splicing regulation. EMBO J. 30, 1965–1976.
[37] Rios, Y., Melmed, S., Lin, S. and Liu, N.A. (2011) Zebrafish usp39 mutation leads to rb1 mRNA splicing defect and pituitary lineage expansion. PLoS Genet. 7, e1001271.

[38] Hao le, T., Burghes, A.H. and Beattie, C.E. (2011) Generation and characterization of a genetic zebrafish model of SMA carrying the human SMN2 gene. Mol. Neurodegener. 6, 24.
[39] Kasher, P.R. et al. (2011) Impairment of the tRNA-splicing endonuclease subunit 54 (tsen54) gene causes neurological abnormalities and larval death in zebrafish models of pontocerebellar hypoplasia. Hum. Mol. Genet. 20, 1574–1584.
[40] Lotti, F. et al. (2012) An SMN-dependent U12 splicing event essential for motor circuit function. Cell 151, 440–454.